

Synchronisation Induced by Repulsive Interactions in a System of van der Pol Oscillators

Teresa VAZ MARTINS^{1,2} and Raúl TORAL¹

¹*IFISC, Instituto de Física Interdisciplinar y Sistemas Complejos, CSIC-UIB,
Campus UIB, E-07122 Palma de Mallorca, Spain*

²*Centro de Física do Porto, DFA, FCUP, 4169-007 Porto, Portugal*

(Received November 13, 2010; Revised July 9, 2011)

We consider a system of identical van der Pol oscillators, globally coupled through their velocities, and study how the presence of competitive interactions affects its synchronisation properties. We will address the question from two points of view. Firstly, we will investigate the role of competitive interactions on the synchronisation among identical oscillators. Then, we will show that the presence of a fraction of repulsive links results in the appearance of macroscopic oscillations at that signal's rhythm, in regions where the individual oscillator is unable to synchronise with a weak external signal.

Subject Index: 034, 055

§1. Introduction

Synchronisation,¹⁾ or the ability of coupled oscillators to adjust their rhythms, is a property that arises in many systems, from pacemaker cells in the heart firing simultaneously as a result of their interaction,²⁾ to the fetal heart rate adjusting its pace to maternal breathing, as an example of forced synchronisation.³⁾

Typically, oscillators with different frequencies are able to synchronise owing to a sufficiently strong positive coupling among units. However, interactions in Nature are often repulsive and, surprisingly, it was found that under some particular circumstances, repulsive interactions can actually enhance synchronisation: thus, the presence of negative links can prevent the instability of the fully synchronised state when it compensates an excessive number of positive links,⁴⁾ or its sparse presence can enhance synchronisation in small-world networks.⁵⁾ Most interestingly — since it is not always desirable to achieve a state of full synchronisation — the presence of repulsive links can give rise to new forms of synchronisation,⁶⁾ which sometimes can be described as glassy or glassy-like,^{7)–10)} or it can lead to clusters of fully phase-synchronised oscillators.¹¹⁾ Additionally, the beam-forming abilities of a system of repulsively coupled Stuart-Landau oscillators were considered in Ref. 12).

Thus far, studies have mostly focused on nonidentical phase oscillators, and several coupling schemes have been chosen, such as local¹³⁾ or long-range,⁵⁾ and purely repulsive⁶⁾ or assuming a competition between repulsive and attractive.¹⁴⁾ Like in Ref. 14), we want to isolate the effect of different proportions of repulsive interactions by considering identical oscillators. However, rather than establishing how full synchronisation becomes unstable as the fraction p of repulsive links increases,¹⁴⁾ our focus will be on the characterisation of the different configurations that emerge as p

grows, and their implications for signal transmission when the system is subjected to an external forcing. Moreover, unlike in Ref. 14), we will not consider phase oscillators, but instead van der Pol oscillators,¹⁵⁾ which implies that phase, amplitude and frequency synchronisation are taken into consideration.

The establishment of the role of the coupling structure on synchronisation, independently of the detailed specification of the nodes dynamics, can rely on the study of the Laplacian matrix.^{16),17)} We will identify and characterise a transition region from synchronisation to desynchronisation by analysing the eigenmodes of the Laplacian matrix corresponding to different proportions of repulsive links, adapting a formalism developed in Refs. 18) and 19).

The second part of the paper will be devoted to exploring the role of competitive interactions in the synchronisation of the system with an external periodic signal. We will choose a signal whose frequency lies outside the region of entrainment for an uncoupled oscillator, as well as for an all attractively coupled system. This problem is closely related to a second theoretical framework, that of resonance studies, which emphasise the importance of an intermediate disorder on the response to a weak signal, where disorder can be noise,^{20),21)} diversity,²²⁾⁻²⁴⁾ or competitive interactions.^{18),25)} In the latter cases^{18),25)} it was found that an intermediate fraction of repulsive links was able to amplify the response to an external signal, in bistable systems where the external signal was the only source of movement. In the present case, an optimal response should correspond to an adjustment between the intrinsic frequency of the oscillators and that of the external signal; as we will see, that optimal response is achieved at an intermediate proportion of repulsive links in the case of strong fast signals, whereas weak slow signals are best responded when all the links are negative.

The outline of this paper is as follows: in §2, we will introduce the model; we show that an increase in the proportion of repulsive links leads to a loss of synchronisation in §3; and in §4, we show how the presence of repulsive links accounts for an enhanced response to external signals; in §5, we will briefly mention some extensions; conclusions are drawn in §6.

§2. Model

We consider an ensemble of van der Pol oscillators¹⁵⁾ $\{x_i(t), i = 1, \dots, N\}$, globally coupled through their velocities \dot{x}_i , and subjected to an external periodic forcing of amplitude A and frequency Ω . The dynamics is described as

$$\ddot{x}_i = -x_i + \mu(1 - x_i^2)\dot{x}_i + \frac{C}{N} \sum_{j=1}^N J_{ij} (\dot{x}_j - \dot{x}_i) + A \sin(\Omega t), \quad (2.1)$$

where the nonlinearity parameter μ is a positive constant and C is the coupling strength.

The coupling between the oscillators i and j is given by the term $J_{ij} = J_{ji}$. As a result of the interaction, the velocity \dot{x}_i of the oscillator i may get closer to that of the oscillator j , or it can get farther apart. In the first case, $J_{ij} = 1$, and we call

the interaction attractive. Otherwise $J_{ij} = -1$ and we call it repulsive. Specifically, we establish the value of J_{ij} according to a given probability p :

$$J_{ij} = J_{ji} = \begin{cases} -1, & \text{with probability } p, \\ 1, & \text{with probability } 1 - p. \end{cases} \quad (2.2)$$

The single van der Pol oscillator is a paradigmatic example of a nonlinear oscillator. It possesses a stable limit cycle as a result of its nonlinear damping term $\mu(1 - x_i^2)$: for small oscillations, $|x_i| < 1$, the system experiences negative damping and the oscillations grow, while for $|x_i| > 1$, the positive damping causes the oscillations to decrease. Therefore, independently of the initial conditions or small perturbations, its amplitude of oscillations reaches a constant (equal to 2), while its detailed shape and period T depend on μ , approaching $T \approx (3 - 2 \ln 2)\mu$ for large μ . In this case of large $\mu \gg 1$, the oscillations are called relaxational and are characterised by the presence of discontinuous jumps intercalated by periods of slow motion.

§3. Desynchronisation among unforced oscillators, $A = 0$

We have numerically solved Eq. (2.1), to investigate the effect of different probabilities of repulsive links. If the initial velocity \dot{x}_i is the same for all units, then the interaction term $J_{ij}(\dot{x}_j - \dot{x}_i)$ is zero and the oscillators evolve independently. The results that follow throughout the paper refer to the case where both x_i and \dot{x}_i are randomly chosen from a uniform distribution on the interval $[-1, 1]$, and we verified that other different random initial conditions produce essentially the same results. Figure 1 shows the trajectory (left panels) and respective limit cycles (right panels) of two typical individual oscillators for some probabilities p of repulsive links. In all the cases, the essential characteristics of the van der Pol oscillator, such as a steady amplitude and the existence of two time scales, are preserved by this type of coupling, as it is reflected by the fact that the stable limit cycles (Fig. 1, right panels) maintain their basic shape. Having identical natural frequencies, when the coupling constant C is sufficiently strong, the position of the oscillators becomes synchronised when all the interactions are attractive (Fig. 1, for $p = 0$). As the proportion of repulsive links grows, both the amplitude and phase of the oscillators start to desynchronise (Fig. 1, $p = 0.4$). Finally, a further increase in the proportion of repulsive links (Fig. 1, $p = 0.60$ and $p = 1.0$) drives the system to a configuration where the global variable $X(t) = \frac{1}{N} \sum_i x_i(t)$ is zero, with several groups oscillating in antiphase, with a decreased frequency and an increased amplitude of oscillations. The examples in Fig. 1 for $p = 0.60$ and $p = 1.0$ illustrate the case of two oscillators that belong to two clusters oscillating in antiphase.

In general, there can be more than one pair of clusters oscillating in antiphase, but we can show that if only one pair of clusters forms such that the oscillators in one cluster are in antiphase with respect to the other, then both clusters have the same number of elements. Consider a cluster consisting of n oscillators with position $x_i = a_i$ and another one of $N - n$ oscillators with position $x_i = -a_i$. The interaction

term between oscillators i and j is given by $J_{ij}(\dot{x}_j - \dot{x}_i) = J_{ij}(\dot{a}_i - \dot{a}_i) = 0$ if they belong to the same cluster, and it is given by $J_{ij}(-2\dot{a}_i)$ if they belong to different clusters. Thus, the evolution equations for two oscillators, each one in a different cluster, are given by

$$\ddot{a}_i = -a_i + \mu(1 - a_i^2)\dot{a}_i + C \left(1 - \frac{n}{N}\right) (2\dot{a}_i)(2p - 1), \tag{3.1a}$$

$$-\ddot{a}_i = a_i - \mu(1 - a_i^2)\dot{a}_i + C \frac{n}{N} (2\dot{a}_i)(1 - 2p), \tag{3.1b}$$

where we have considered that the fraction of repulsive and attractive links is the same for both oscillators, that is, we have neglected the variance in the binomial distribution, an approximation that improves with increasing system size N . For (3.1a) and (3.1b) to hold simultaneously, we must have $n = \frac{N}{2}$. Hence, the clusters have the same number of elements, and therefore, the average position of the system, $X(t)$, is zero.

We use this result — considering two clusters with the same number n of elements — to compute, in the case $p = 1.0$, the increase in the amplitude of a single oscillator. Defining $b_i(t) \equiv \frac{a_i(t)}{\sqrt{1 + \frac{C}{\mu}}}$, and setting $p = 1.0, n = \frac{N}{2}$, in (3.1a), we find that $b_i(t)$ satisfies the van der Pol equation:

$$\ddot{b}_i = -b_i + \tilde{\mu}(1 - b_i^2)\dot{b}_i \tag{3.2}$$

with $\tilde{\mu} = \mu + C$. The amplitude of $b_i(t)$ tends to $|b_i| = 2$, and, hence, the amplitude of oscillations of the original variable is $|a_i| = |b_i|\sqrt{1 + \frac{C}{\mu}} = 2\sqrt{1 + \frac{C}{\mu}}$. For $\mu = 10$ and $C = 20$, the predicted amplitude is $a_i = 3.46$, as we can observe in the left panel of Fig. 1 for $p = 1.0$.

We can describe the last configuration characterised by a zero value of the average position $X(t)$ as a disordered situation at the macroscopic level in the sense that

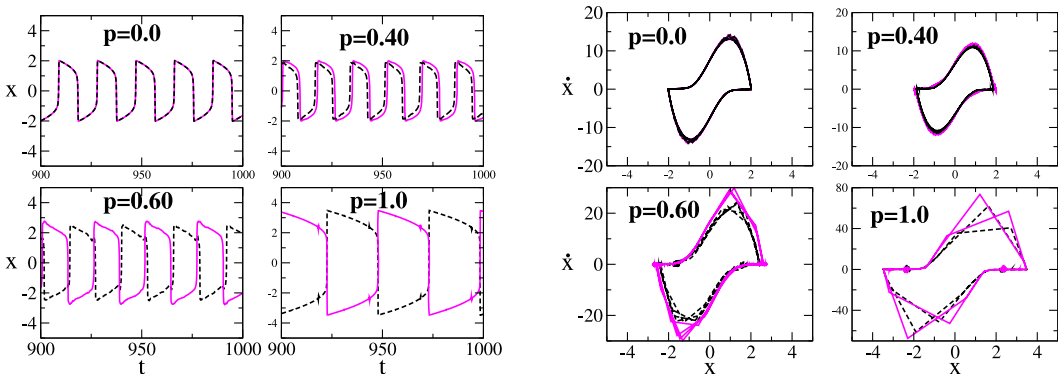


Fig. 1. Trajectories (left panels) and phase portraits (right panels) of two individual oscillators, for various probabilities p of repulsive links. Regardless of initial conditions, the van der Pol oscillator reaches steadystate oscillations with a constant amplitude. In the right panel, we represent the corresponding limit cycles in the phase plane of (x, \dot{x}) : as p grows, the distinction between slow and fast motions becomes clearer which is manifested in the more abrupt angles in the limit cycles for $p = 0.6$ and $p = 1.0$. $N = 100, C = 20, \mu = 10, A = 0$.

the oscillators are desynchronised in relation to the average position, although there are several clusters of oscillators synchronised amongst themselves. To quantify this *disordering* role of repulsive links, we define, following Ref. 24), the complex variable $z_i = x_i + i\dot{x}_i$, the average $\bar{z} = \frac{1}{N} \sum_{i=1}^N z_i$ and the variance of z_i normalised by the average value of the modulus squared, $\sigma^2[z_i]$:

$$\sigma^2[z_i] = \left\langle \frac{N^{-1} \sum_{i=1}^N |z_i - \bar{z}|^2}{N^{-1} \sum_{i=1}^N |z_i|^2} \right\rangle, \quad (3.3)$$

here and henceforth, $\langle \dots \rangle$ denotes a time average.

The normalised variance can take values between $\sigma^2[z_i] = 1$ for maximum disorder, and $\sigma^2[z_i] = 0$ when all oscillators are synchronised amongst themselves. From this, we choose²⁴⁾ a measure of order that reduces to the Kuramoto order parameter²⁶⁾ when all units oscillate with the same amplitude:

$$\rho = \sqrt{1 - \sigma^2[z_i]}. \quad (3.4)$$

As dispersion increases, ρ decreases from $\rho = 1$ to $\rho = 0$. As we show in Fig 2, there is a clear synchronisation-desynchronisation transition for an intermediate fraction of repulsive links, which does not depend much on the coupling strength C .

To characterise the desynchronisation further, it is useful to look into the behaviour of the field that an oscillator feels as a result of the interaction with other units. The average number of *effective links* $F = \frac{1}{N^2} \sum_{ji} J_{ij}$, in a given run can in general be different from the particular number an oscillator has, $f_i = \frac{1}{N} \sum_{j=1}^N J_{ij}$, given that the probability of repulsive links p follows a binomial distribution with the corresponding variance.

We want to know if there is a correlation between the fraction of repulsive links an oscillator has and its synchronisation with the overall majority. That is described by the following quantity G :

$$G = \left\langle \frac{1}{N} \sum_{ji} \dot{x}_j \dot{x}_i [f_i - F] \right\rangle = \left\langle \dot{X} \sum_i \dot{x}_i [f_i - F] \right\rangle, \quad (3.5)$$

with $\dot{X} = \frac{1}{N} \sum_j \dot{x}_j$ being the mean velocity. We observe that the order-disorder transition region $p \sim [0.4, 0.45]$ which we identify in the left panel of Fig. 2, is accompanied by an increase in the influence on an oscillator of its particular coupling configuration, as signalled by the peak in G (Fig. 2, right panel). The oscillators with a higher than average number of repulsive links form a loosely synchronised group in a different slow region than the one where the majority concentrates.

The partial independence of the state of the oscillator on the global configuration opens the possibility of the existence of several different global states, and thus hints at the existence of metastable states. We can relate this behaviour to the coupling structure, by the spectral analysis of the associated Laplacian matrix $J'_{ij} = J_{ij} - \delta_{ij} \sum_{k=1}^N J_{kj}$,¹⁸⁾ where δ_{ij} is Kronecker's delta. We begin by rewriting Eq. (2.1) as a system of two equations that highlight a fast motion for the x_i variable and a slow motion for the y_i variable:

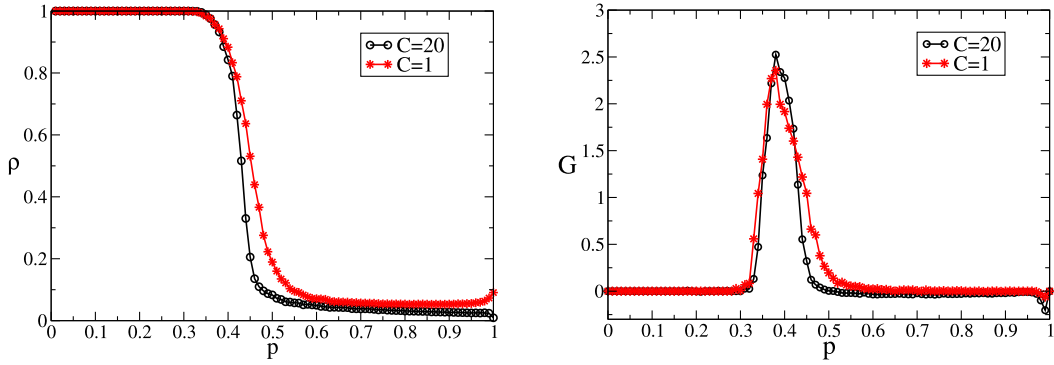


Fig. 2. Measures of disorder ρ , Eq. (3.4), (left panel) and G , Eq. (3.5), (right panel). Averages over 100 runs, and N , μ and A as in Fig. 1.

$$\dot{x}_i = \mu \left[x_i - \frac{1}{3}x_i^3 - y_i + \frac{D}{N} \sum_{j=1}^N J'_{ij}x_j \right], \tag{3.6a}$$

$$\dot{y}_i = \frac{1}{\mu} [x_i - A \sin(\Omega t)], \tag{3.6b}$$

where $D = \frac{C}{\mu}$.

We focus on Eq. (3.6a), letting the slow variable y_i be a constant. We now introduce the eigenvalues Q_α and eigenvectors $e^\alpha = (e_1^\alpha, \dots, e_N^\alpha)$ of the Laplacian matrix, with the normalisation condition $\sum_i e_i^\alpha e_i^\beta = \delta_{\alpha\beta}$,

$$\sum_{j=1}^N J'_{ij}e_j^\alpha = Q_\alpha e_i^\alpha. \tag{3.7}$$

Let us assume that the state of a unit i is x_i^o at a given time, where x_i^o is randomly drawn from an even distribution, such that the average $\frac{1}{N} \sum_{i=1}^N x_i^o = 0$, all the odd moments about the mean are zero, and the variance of the distribution is $\frac{1}{N} \sum_{i=1}^N (x_i^o)^2$. We perturb the initial states as $x_i^o + s_i$, and express the perturbation s_i in the eigenbasis of the Laplacian, so that

$$s_i = \sum_{\alpha=1}^N B_\alpha e_i^\alpha. \tag{3.8}$$

We aim to see how the interaction with other units affects the reaction to perturbations, in particular, for the intermediate values of the proportion of repulsive links.

After expanding Eq. (3.6a) in the eigenbasis of the Laplacian, we then multiply the resulting equation by e_i^α and average over all elements i . Given that the eigenvectors e_i^α are independent of the initial conditions x_i^o , we will assume for simplification that $\frac{1}{N} \sum_{i=1}^N x_i^o e_i^\alpha \sim \frac{1}{N^2} \sum_{i=1}^N x_i^o \sum_{i=1}^N e_i^\alpha = 0$. The evolution equation for

the amplitude of the α -th mode becomes

$$\frac{1}{\mu} \frac{dB_\alpha}{dt} = -\frac{1}{3} \sum_{i=1}^N \sum_{\beta, \gamma, \eta} e_i^\beta e_i^\gamma e_i^\eta e_i^\alpha B_\beta B_\gamma B_\eta + \left(\frac{C Q_\alpha}{\mu N} - k \right) B_\alpha, \quad (3.9)$$

where $k \equiv \frac{1}{N} \sum_{i=1}^N (x_i^o)^2 - 1$ is a quantity related to the variance of the initial conditions.

From this equation, we see that the positive Laplacian eigenvalues Q_α contribute to the growth of the amplitude of perturbations.^{(17), (18)} Therefore, it is useful to see how different probabilities of repulsive links affect the eigenvalues and the characteristics of the respective eigenvectors. The participation ratio $\text{PR}_\alpha = 1 / \sum_{i=1}^N [e_i^\alpha]^4$ is a classical measure of localisation,^{(28), (29)} which estimates the number of oscillators that participate significantly in a state e^α : for a state localised on a fraction f of elements, PR_α tends to f .

In the left panel of Fig. 3 we plot the participation ratio PR_α as a function of the Laplacian eigenvalues Q_α for some probabilities p of repulsive links. While for extreme probabilities p of repulsive links, the number of possible values for Q_α is very restricted, we find that for intermediate levels of p , the distribution of Q_α is broader and the eigenvalues at both tails of the spectrum are more localised. We also note that as p increases, the eigenvalues become dislocated towards higher values, and when $p = 0.5$, there are as many positive as negative possible eigenvalues. For values of p that coincide with the transition from synchronisation to desynchronisation seen in Fig. 2, there exists a significant number of positive eigenvalues that have a low participation ratio, which is illustrated for $p = 0.42$ in Fig. 3. This is understandable when we remember that the transition region is characterised by a heightened dependence of the state of an oscillator on its particular coupling structure (Fig. 2, right panel), which determines that some oscillators are more synchronised than others, which is another way of saying that the disorder is localised.

However, the contribution of the coupling term to the maintainance of a perturbed state may not be sufficient to avoid the decay to the initial state. Even when the eigenvalues are positive, B_α can be zero depending on the sign and magnitude of the several terms in Eq. (3.9), which varies for different realisations of the Laplacian matrix. On a first approximation, that is mostly valid for localised modes and does not hold in every case,⁽¹⁹⁾ we can neglect the coupling between modes, assuming that $\sum_{i=1}^N e_i^\beta e_i^\gamma e_i^\eta e_i^\alpha \approx 0$ unless $\beta = \gamma = \eta = \alpha$. The equation for an uncoupled α -mode becomes

$$\frac{\text{PR}_\alpha}{\mu} \frac{dB_\alpha}{dt} = -\frac{1}{3} B_\alpha^3 + \text{PR}_\alpha \left(\frac{C Q_\alpha}{\mu N} - k \right) B_\alpha. \quad (3.10)$$

According to Eq. (3.10), unless $Q_\alpha > \frac{kN\mu}{C}$, B_α tends to zero, and any deviation from the initial state vanishes. Otherwise, mode α is said to be an *open mode*.

To concretise the impression left by the observation of the left panel of Fig. 3, that the transition region $p \approx 0.42$ seems to correspond to a localisation of positive modes (those with an associated positive eigenvalue), we will define ‘‘localised’’ modes as the ones whose participation ratio is less than $0.1N$, and define a measure M of

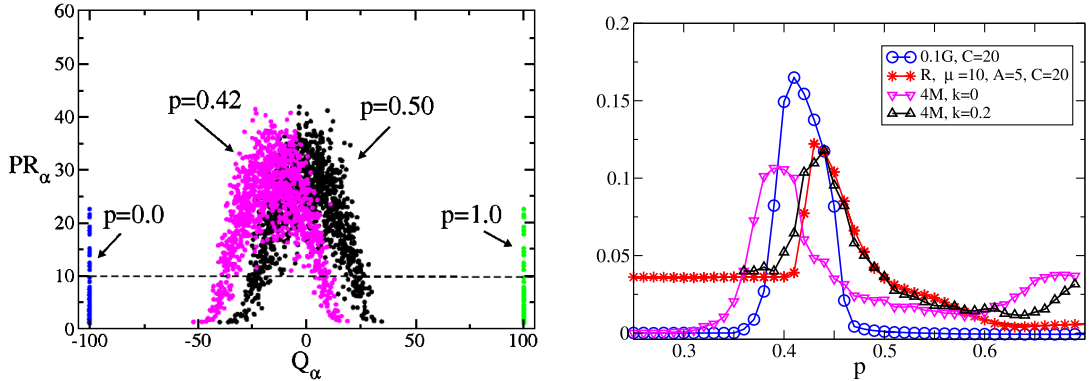


Fig. 3. Left panel: we plot the participation ratio PR_α for the Q_α eigenvalues. As the probability of repulsive links p grows, the eigenvalues become dislocated towards higher values. The eigenvalues whose participation ratio is below the dashed line are localised. Right panel: the measures of localisation M , the measure of disorder G , and the spectral power amplification R , all have the maximum value at roughly the same p . For better viewing, we multiplied M by 4, and G by 0.1. $N = 100$. In the case of M and $k = 0.2$, we have $C = 20$ and $\mu = 10$.

localisation¹⁸⁾ as $M = \frac{N_L^2}{N_O N}$, where N_L is the number of positive open localised modes, i.e., those satisfying $PR_\alpha < 0.1N$, and N_O is the total number of positive open modes. This measure takes its maximal value for the probability that has the greatest number of localised positive open modes, and no extended positive open mode.

As we see in the right panel of Fig. 3, the peak in G (Eq. (3.5)), which signals the transition region (Fig. 2), coincides with a localisation of the open modes of the Laplacian when we consider small enough variances, or $k \approx 0$. As expected, the results obtained from the numerical simulation of Eq. (2.1) do not show such a dependence on the initial conditions as observed in this bistable approximation, since the position of the oscillators is always changing with time. Arguably, the consideration of the effect of coupled modes would allow for a more precise coincidence with a lesser dependence of the opening of modes on the initial conditions.

§4. Synchronisation with the external signal, $A \neq 0$

In this section, we will see how competitive interactions affect the response to an external periodic signal. Since in general there can be several frequencies present in the output of the global variable $X(t) = \frac{1}{N} \sum_i x_i(t)$, we say that the system is synchronised with the external signal when the highest peak in the Fourier spectrum corresponds to that frequency.

When the natural frequency of oscillations coincides with the external forcing frequency, synchronisation is achieved for vanishing A , and as the two frequencies diverge, stronger forcing are needed to entrain the system. We will call a signal *strong* when its amplitude is greater than the amplitude of oscillation of the unforced van der Pol unit, and we will call it *fast* when its frequency is higher than the natural frequency of the individual van der Pol oscillator. In the case of coupled oscillators

with some proportion of repulsive links, a slow signal can in general be more easily followed by the system: a weak fast signal does not have time to have any effect regardless of the proportion of repulsive links, while a strong slow signal is more easily responded even without the presence of repulsive links. Therefore, we will not consider these cases.

We will distinguish between strong fast and weak slow signals, because the mechanism of synchronisation differs in the two cases, although, in both cases, competitive interactions are required for an enhanced response.

4.1. Strong fast signals benefit from intermediate p

In Fig. 4, we plot the synchronisation regions and their relative strength, as measured by the spectral power amplification factor²⁷⁾ R , given by

$$R = 4A^{-2} |\langle e^{-i\Omega t} X(t) \rangle|^2. \quad (4.1)$$

R is roughly proportional to the square of the normalised amplitude of the oscillations of $X(t)$ at the frequency Ω , being $R < 1$ when the amplitude of oscillations of the forced system is smaller than the amplitude of the external signal.

When $p = 0$ (Fig. 4, left panel), the synchronisation region with respect to the frequency Ω and amplitude A of the external signal has the typical triangular-like shape seen on Arnold tongues.¹⁾ An intermediate fraction of repulsive links ($p = 0.43$, Fig. 4, right panel) pushes the synchronisation borders beyond the $p = 0$ values, allowing for synchronisation of faster signals at weaker forcing.

Figure 5 shows the steady-state trajectory of the macroscopic variable $X(t)$, for different probabilities p of repulsive links, and illustrates the fact that a certain proportion of repulsive links is required for the system to adjust its rhythm to that of the external signal (Fig. 5, $p = 0.40$), whereas Fig. 6 confirms that this optimal response only occurs for an intermediate range of the probability of repulsive links. It should be noted that when entrained, the oscillators adjust their frequency while

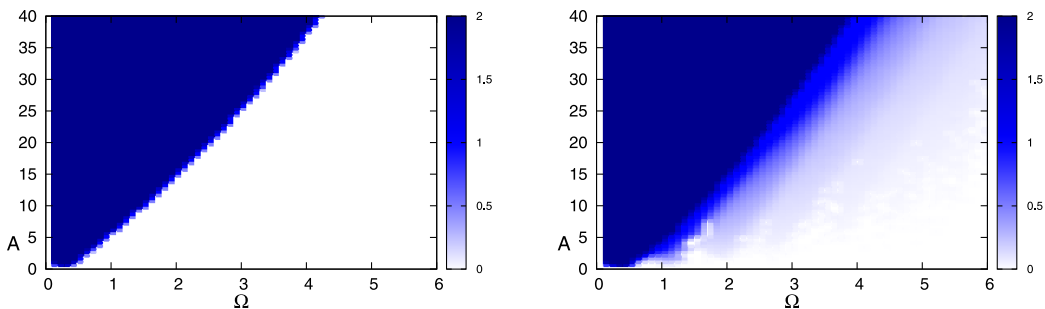


Fig. 4. We plot the spectral power amplification R in the synchronisation regions for $p = 0$ (left panel) and $p = 0.43$ (right panel), when the natural frequency of the oscillator is ≈ 0.39 . For better viewing, we use a color code that saturates for $R \geq 2$. N, C and μ as in Fig. 1.

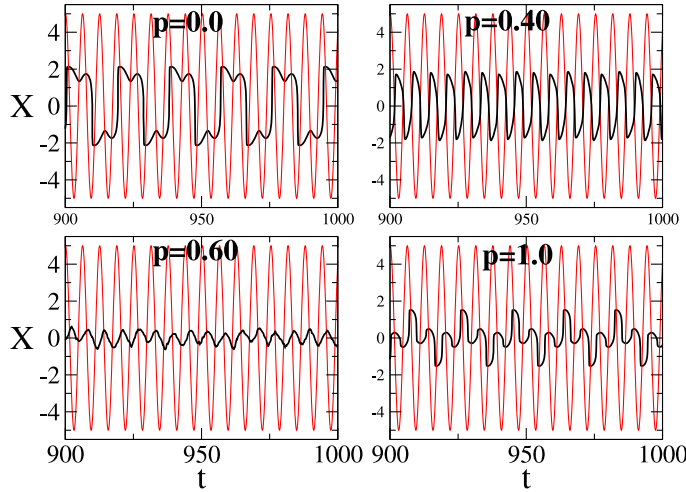


Fig. 5. Time evolution of the macroscopic variable $X(t)$ when the system is forced by an external sinusoidal fast signal (lighter color) of amplitude $A = 5$ and frequency $\Omega = 1.0$, for several probabilities of repulsive links p . N, C and μ as in Fig. 1.

keeping their natural amplitude (Fig. 5); therefore, the spectral amplification factor R is smaller than 1, when $A > 2$. As expected, the more the natural frequency deviates from the forcing frequency, the stronger the signal needs to be in order to entrain the system: namely (Fig. 6), for a forcing frequency $\Omega = 1$, the signal strength needs to be $A = 12$ instead of $A = 5$, when the natural frequency $\omega = 2\pi/T$ is ≈ 0.19 ($\mu = 20$) instead of ≈ 0.39 ($\mu = 10$).

To understand the significance of competitive interactions, we recall the results of the last section. The region of p where the system can be entrained by fast signals

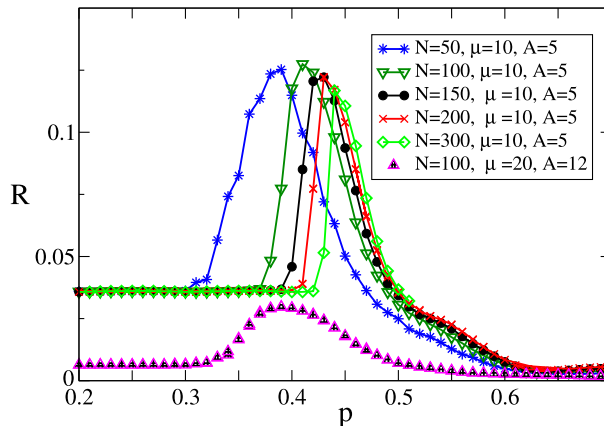


Fig. 6. Spectral power amplification, for $C = 20$, $\Omega = 1$ and several system sizes N , averages over 100 runs. We note that smaller systems become synchronised at lower fractions of repulsive links, and are not so dependent on the precise fraction of repulsive links. Additionally, we also observed (figures not shown) a resonance with system size for different probabilities of repulsive links. This kind of dependence has been explained elsewhere.¹⁸⁾

is signalled by the peak in the spectral power amplification R , and coincides with the localisation region, as given by the peak in M (Fig. 3).

This localisation is crucial for an enhanced response to fast signals, because disorder places some units in a position where they can be affected by the signal and then pull some of the other oscillators to whom they are attractively coupled, but the fact that it is localised allows for a coherence of the collective motion.

4.2. Weak slow signals benefit from very high p

In the previous section, we chose to measure the enhancement at the collective level, using the macroscopic variable $X(t)$ in our measure of response R , Eq. (4.1); that corresponded to a synchronisation with the external forcing at the individual level: the greater the number of entrained oscillators, the greater the response.

We find a different situation when we subject our system to a weak slow signal, say $A = 0.9$. A complete amplitude and frequency synchronisation with this forcing would imply a fast motion, in the interval $[-1, 1]$, without any intercalating period of slow motion, thus basically destroying the defining feature of a relaxational oscillator (§2). We find it impossible for such a weak signal to entrain an individual oscillator. Yet, we observe that for a sufficiently high fraction of repulsive links (insets of Figs. 7 and 8), there is a near coincidence between the trajectory of the global variable $X(t)$ and the forcing $A \sin(\Omega t)$, with an almost imperceptible phase delay. Therefore, the simplest measure of entrainment, which falls to zero if there is a perfect synchronisation, is

$$D = \frac{\langle [X(t) - A \sin(\Omega t)]^2 \rangle}{\langle X(t)^2 \rangle}. \quad (4.2)$$

The results plotted in Fig. 7 show that as the probability of repulsive links increases, the system becomes synchronised with the external signal. Most interestingly, this synchronisation with the external signal mirrors the loss of synchronisation amongst oscillators seen in Fig. 2 for the unforced system. In fact, the mechanism responsible for the synchronisation that appears when the fraction of repulsive links is high has its roots in the existence of groups oscillating in antiphase in the unforced system. These antiphase oscillations are visible in the illustrative examples plotted in Fig. 1 for $p = 0.6$ and $p = 1.0$, and in the lower-right panel of Fig. 8 when the value of the periodic signal is zero. When the signal amplitude begins to increase, there appears an asymmetry in the oscillations favouring the time spent on the slow branch region that is closer to the value of the signal, as seen in the lower panels of Fig. 8.

While the individual waves get cancelled when units are oscillating in antiphase, the longer time spent on the slow branch whose value is closer to the signal's causes the superposition of the individual waves in that zone (see right panel of Fig. 8 for $p = 1.0$). As a result, the global variable becomes synchronised with the external forcing, even if the individual oscillators are not.

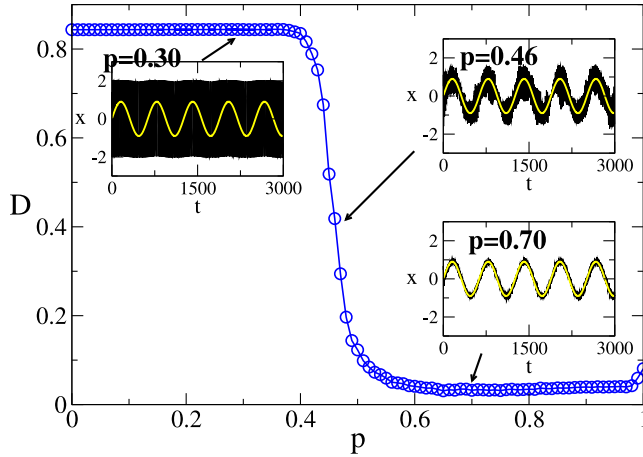


Fig. 7. Illustration of representative macroscopic trajectories: a weak slow signal is best followed the more repulsive connections it has. Other parameters: $A = 0.9$, $\Omega = 0.01$. N, C and μ as in Fig. 1.

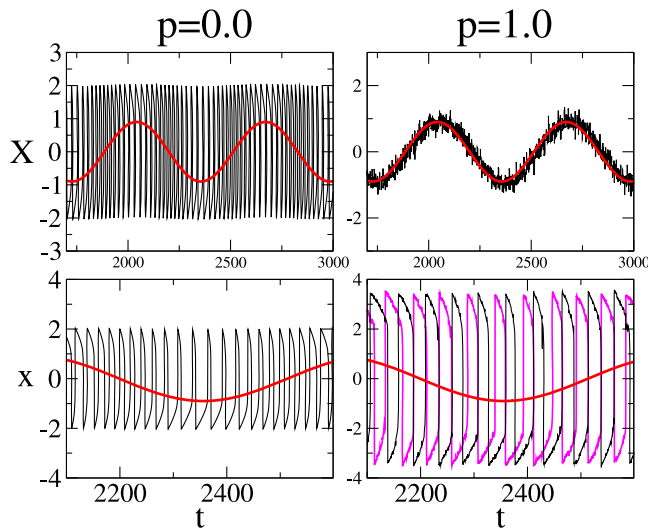


Fig. 8. The slower oscillation corresponds to the external signal, while the higher frequency oscillations correspond to either the trajectory of the macroscopic variable $X(t)$ or two typical individual trajectories. Upper panels: When $p = 1.0$, we observe the synchronisation of the macroscopic variable with a signal that is weak and slow. Lower panels: we zoom and plot two representative individual trajectories. $A = 0.9$, $\Omega = 0.01$. N, C and μ as in Fig. 1.

§5. Further applications: FitzHugh-Nagumo

The single uncoupled van der Pol oscillator can be transformed either into a linear oscillator by taking $\mu = 0$ or by replacing the nonlinear damping term $\mu(1-x_i^2)$, Eq. (2.1) by a constant, or into an excitable system — a simplified FitzHugh-Nagumo

— by adding a constant a such that $|a| > 1$ to Eq. (3.6b) so that the system becomes

$$\dot{x}_i = \mu \left[x_i - \frac{1}{3}x_i^3 - y_i + \frac{D}{N} \sum_{j=1}^N J'_{ij}x_j \right], \quad (5.1a)$$

$$\dot{y}_i = \frac{1}{\mu} [x_i - A \sin(\Omega t) + a]. \quad (5.1b)$$

Thus, a first direct extension consists of a brief exploration of how those transformations affect our results. Not surprisingly, we did not find an enhanced response for linear oscillators: both mechanisms of enhancement for slow and fast signals rely on the existence of a slow motion region. This situation contrasts with the case studied in Ref. 24). In that paper, the authors studied a system of linear oscillators with a distribution of natural frequencies. Defining as a measure of diversity the variance of the natural frequencies, they found an optimal response to an external signal for an intermediate level of diversity. Interestingly enough, the enhancement of response also had its origins in an intermediate level of disorder. However, the microscopic mechanism was rather different: some oscillators had a natural frequency that resonated with the signal's frequency, and were able to pull the others due to the positive coupling. In our case, there is no single oscillator whose frequency can be entrained by the external signal. On the other hand, the mechanisms we proposed should be applicable to the FitzHugh-Nagumo model.

The interaction via competitive interactions can play the same role as noise or diversity, thus enabling rhythmic excursions away from the fixed point. The result shown in Fig. 9 bears some resemblance to the phenomenon by which we observe that the periodicity of oscillations becomes maximally ordered for an intermediate level of noise,^{31)–33)} diversity,³⁴⁾ or competitive interactions.^{5),36)} In our case, however, and as it was observed in Ref. 35) for the case of active rotators, we do not observe any oscillations at all unless some interactions are repulsive.

When we force the excitable system with a sufficiently strong fast signal (Fig. 10), it starts to oscillate even for $p = 0$, and for an intermediate amount of repulsive interactions, the main frequency of oscillations coincides with the external signal (Fig. 10, $p = 0.40$).

On the other hand, when we force a system of FitzHugh-Nagumo elements with slow weak signals (Fig. 11), we observe bursts with the periodicity of the signal for $p = 0$, while for $p = 1$, the global variable roughly oscillates along with the external forcing. Even though the periodicity of the external signal is detected for all the fractions of repulsive links, we can imagine situations where we actually want to replicate the behaviour of the external signal, and that is only possible when the fraction of repulsive links is sufficiently large. Both of these results are expected taking into account the arguments we gave for the van der Pol oscillator case.

§6. Conclusions

We have shown that the presence of repulsive links in a system of globally coupled van der Pol oscillators can enhance the response to an external signal. This

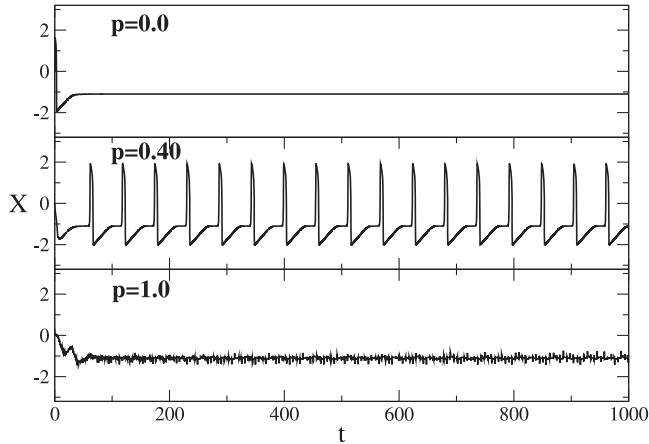


Fig. 9. Trajectory of the global variable X for different fractions of repulsive links p in the unforced FitzHugh-Nagumo system showing a similar phenomenon to coherence resonance. Other parameters: $a = 1.1$, N, C and μ as in Fig. 1.

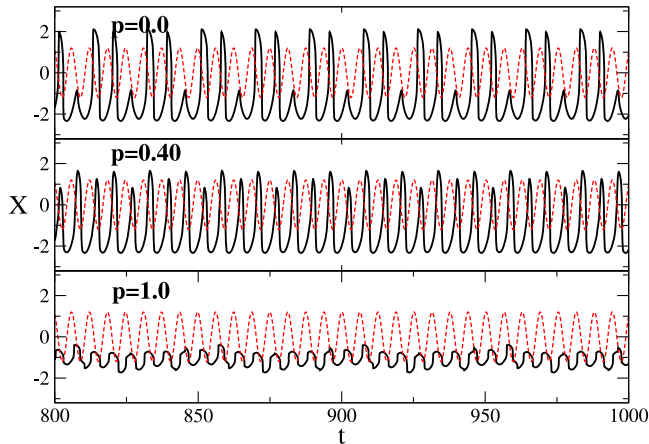


Fig. 10. Trajectories of the global variable X for a system of FitzHugh-Nagumo units in the excitable regime forced by a fast signal, for increasing fractions of repulsive links p . Other parameters: $a = 1.1$, $A = 12$, $\Omega = 1$, N, C and μ as in Fig. 1. The pointed line shows the external signal multiplied by 0.1, for better viewing.

phenomenon is verified regardless of whether the signal is strong and fast, or weak and slow, and it is in every case directly related to a loss of synchronisation and the existence of a slow-motion region, but the *microscopic* mechanism of enhancement is different in each case.

From the point of view of a strong fast signal, the van der Pol oscillator can be approximated by a bistable system, implying a threshold that is regularly overcome with the help of an intermediate proportion of repulsive links, by means of the deformation of the slow-motion region. In the case of very slow signals, the mechanism is associated with the tendentially antiphase oscillations that occur when there is

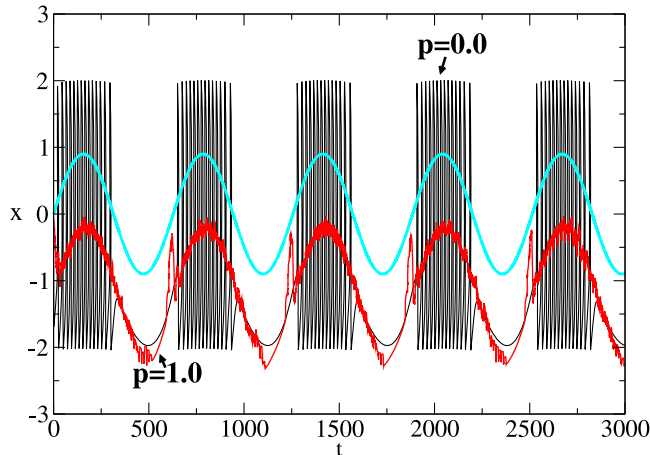


Fig. 11. Representative trajectories of the global variable for a system of FitzHugh-Nagumo units in the excitable regime, $a = 1.1$, for some probabilities p of repulsive links. Other parameters: $\Omega = 0.01$, $A = 0.9$, and N , C and μ as in Fig. 1. The signal is represented in a lighter color.

a majority of repulsive links.

In both cases, the enhancement is directly related to a loss of full synchronisation when the fraction of repulsive links increases. One can imagine that a different coupling scheme may enhance or hinder the results we found, since it is known that the network topology plays a role in synchronisation properties.³⁷⁾

Acknowledgements

We acknowledge financial support from the MICINN (Spain) and FEDER (EU) through project FIS2007-60327 (FISICOS). TVM is supported by FCT (Portugal) through Grant No. SFRH/BD/23709/2005.

References

- 1) A. Pikovsky, M. Rosenblum and Jürgen Kurths, *Synchronisation: A Universal Concept in Nonlinear Sciences* (Cambridge Univ. Press, Cambridge, 2003).
- 2) J. Jalife, *J. Physiol.* **356** (1984), 221.
- 3) P. Van Leeuwen, D. Geue, M. Thiel, D. Cysarz, S. Lange, M. C. Romano, N. Wessel, J. Kurths and D. H. Grönemeyer, *Proc. Natl. Acad. Sci. USA* **106** (2009), 13661.
- 4) T. Nishikawa and A. E. Motter, *Proc. Natl. Acad. Sci. USA* **107** (2010), 10342.
- 5) I. Leyva, I. Sendiña-Nadal, J. A. Almendral and M. A. Sanjuan, *Phys. Rev. E* **74** (2006), 056112.
- 6) L. S. Tsimring, N. F. Rulkov, M. L. Larsen and M. Gabbay, *Phys. Rev. Lett.* **95** (2005), 014101.
- 7) H. Daido, *Prog. Theor. Phys.* **77** (1987), 622.
- 8) H. Daido, *Phys. Rev. Lett.* **68** (1992), 1073.
- 9) H. Daido, *Phys. Rev. E* **61** (2000), 2145.
- 10) L. L. Bonilla, C. Pérez-Vicente and J. M. Rubí, *J. Stat. Phys.* **70** (1993), 921.
- 11) K. Okuda, *Physica D* **63** (1993), 424.
- 12) N. F. Rulkov, L. Tsimring, M. L. Larsen and M. Gabbay, *Phys. Rev. E* **74** (2006), 056205.
- 13) M. Giver, Z. Jabeen and B. Chakraborty, *Phys. Rev. E* **83** (2011), 046206.
- 14) D. H. Zanette, *Europhys. Lett.* **72** (2005), 190.

- 15) B. van der Pol and J. van der Mark, London Edinburgh Dublin Philos. Mag. J. Sci. Ser. 7, **6** (1928), 763.
- 16) L. M. Pecora and L. T. Carroll, Phys. Rev. Lett. **80** (1998), 2109.
- 17) P. N. McGraw and M. Menzinger, Phys. Rev. E **77** (2008), 031102.
- 18) T. Vaz Martins, V. N. Livina, A. P. Majtey and R. Toral, Phys. Rev. E **81** (2010), 041103.
- 19) M. Perc, M. Gosak and S. Kralj, Soft Matter **4** (2008), 1861.
- 20) L. Gammaitoni, P. Hänggi, P. Jung and F. Marchesoni, Rev. Mod. Phys. **70** (1998), 223.
- 21) *Topical Issue on Stochastic Resonance*, ed. P. Hänggi and F. Marchesoni, Eur. Phys. J. B **69** (2009), Special Issue.
- 22) C. Tessone, C. R. Mirasso, R. Toral and J. D. Gunton, Phys. Rev. Lett. **97** (2006), 194101.
- 23) R. Toral, C. J. Tessone and J. Viana Lopes, Eur. Phys. J. Special Topics **143** (2007), 59.
- 24) R. Toral, E. Hernandez-Garcia and J. D. Gunton, Int. J. Bifurcation Chaos **19** (2009), 3499.
- 25) T. Vaz Martins, R. Toral and M. A. Santos, Eur. Phys. J. B **67** (2009), 329.
- 26) Y. Kuramoto, *Chemical Oscillations, Waves and Turbulence* (Springer-Verlag, New York, 1984).
- 27) P. Jung and P. Hänggi, Europhys. Lett. **8** (1989), 505.
- 28) P. W. Anderson, Phys. Rev. **109** (1958), 1492.
- 29) P. W. Anderson, Mater. Res. Bull. **5** (1970), 549.
- 30) J. Restrepo, E. Ott and B. Hunt, Phys. Rev. Lett. **93** (2004), 114101.
- 31) A. S. Pikovsky and J. Kurths, Phys. Rev. Lett. **78** (1997), 775.
- 32) A. Neiman, L. Schimansky-Geier, A. Cornell-Bell and F. Moss, Phys. Rev. Lett. **83** (1999), 4896.
- 33) C. Kurrer and K. Schulten, Phys. Rev. E **51** (1995), 6213.
- 34) C. J. Tessone, A. Scirè, R. Toral and P. Colet, Phys. Rev. E **75** (2007), 016203.
- 35) C. J. Tessone, D. H. Zanette and R. Toral, Eur. Phys. J. B **62** (2008), 319.
- 36) J. A. Almendral, I. Leyva and I. Sendiña-Nadal, Int. J. Bifurcation Chaos **19** (2009), 711.
- 37) A. Arenas, A. Díaz-Guilera, J. Kurths, Y. Moreno and C. Zhou, Phys. Rep. **469** (2008), 93.